Research Article

Xiaozhen He, Ilkka Rytöluoto, Rafal Anyszka, Amirhossein Mahtabani, Minna Niittymäki, Eetta Saarimäki, Christelle Mazel, Gabriele Perego, Kari Lahti, Mika Paajanen, Wilma Dierkes*, and Anke Blume

Combining good dispersion with tailored charge trapping in nanodielectrics by hybrid functionalization of silica

https://doi.org/10.1515/epoly-2021-0054
received March 04, 2021; accepted June 24, 2021

Abstract: Fumed silica-filled polypropylene (PP)-based nanodielectrics were studied in this work. To not only improve the dispersion of the silica but also introduce deep charge traps into the polymeric matrix, five types of modified silicas were manufactured with different surface modifications. The modified silica surfaces comprise an inner and a surface layer. The inner layer contains a polar urethane group for tailoring the charge trap properties of the PP/propylene–ethylene copolymer nanocomposites, whereas the surface layer consists of hydrocarbons (ethyl-, *tert*-butyl-, cyclopentyl-, phenyl-, or naphthalenyl moieties) in order to gain a good dispersion of the silica in the unpolar polymer blend. Scanning electron microscopic pictures proved that these tailored silicas show a much better dispersion than the unmodified one. Thermally stimulated depolarization current measurements revealed the ability of the silica to introduce deep charge traps with low trap density. The trap depth distribution depends on the type of the unpolar surface layer consisting of the different hydrocarbons. Among these five differently modified silicas, the introduction of the one with a surface layer consisting of *tert*-butyl moieties resulted in the lowest charge injection and the lowest charge current in the nanocomposite, proving good dielectric performance. Additionally, this silica exhibits good dispersion in the polymeric matrix, indicating a promising performance for nanodielectric application.

Keywords: fumed silica, surface functionalization, charge trap distribution, nanodielectrics

*** Corresponding author: Wilma Dierkes,** University of Twente, Faculty of Engineering Technology, Department of Mechanics of Solids, Surfaces and Systems (MS3), Chair of Elastomer Technology and Engineering, 7522 NB, Enschede, The Netherlands, e-mail: w.k.dierkes@utwente.nl
Xiaozhen He, Rafal Anyszka, Amirhossein Mahtabani, Anke Blume: University of Twente, Faculty of Engineering Technology, Department of Mechanics of Solids, Surfaces and Systems (MS3), Chair of Elastomer Technology and Engineering, 7522 NB, Enschede, The Netherlands
Ilkka Rytöluoto, Eetta Saarimäki, Mika Paajanen: VTT Technical Research Centre of Finland Ltd, FI-33720, Tampere, Finland
Minna Niittymäki, Kari Lahti: Tampere University, High Voltage Engineering, 33100, Tampere, Finland
Christelle Mazel, Gabriele Perego: Nexans Research Center, 29 Rue Pré Gaudry, 69007 Lyon, France

1 Introduction

The term “nanodielectrics” describes a nanocomposite designed for maximized dielectric performance. The definition of a “nanocomposite” is a composite filled with nanoparticles, of which at least one dimension is lower than 100 nm. The nanodielectrics designed for application in high-voltage fields require high electrical insulation properties to effectively fulfill this task. Early studies with promising results were published in 2002 by Nelson and his coauthors (1). They reported that the nanoparticles can delay the charge transportation and reduce the space charge accumulation, which indicates the potential of the nanoparticles for dielectric applications. Since then, nanodielectrics have attracted ever-increasing attention (2,3). Subsequently, a lot of effort was spent on understanding the effect of these fillers in nanodielectrics (4,5). The large interfacial area between the nanofiller surface and polymer matrix is widely accepted to be one of the most important factors that greatly impact the performance of nanodielectrics. The nanofiller not only alters the polymer chain dynamics and the chain mobility at the interface region (6) but also brings various chemical functional groups into this area, tailoring the charge trapping properties of the nanocomposite (7).

Good adhesion between the well-dispersed nanofiller and the polymer matrix is considered to be the most important feature of high voltage direct current (HVDC) cable insulation materials (8). During the installation of a high-voltage cable, the cable is under mechanical stress and strain. Poor nanofiller-polymer adhesion or the presence of nanofiller aggregates might cause the formation of cavities under strain, which can lead to microcrack formation and subsequently mechanical failure. This might also affect the dielectric performance of the nanocomposite. Moreover, introducing a polar functional group on the nanofiller surface can provide a positive effect on the dielectric performance due to the introduced deep charge traps (9).

In general, the most commonly used polymers for HVDC insulation are crosslinked polyethylene (XLPE) and polypropylene (PP). Due to the crosslinked nature of the XLPE, it is not recyclable. Driven by the focus on sustainability, PP is a potential candidate for replacing XLPE in the future due to its recyclable character. However, XLPE and PP are both unpolar polymers. Considering the need of a good dispersion of a nanofiller in an unpolar polymeric matrix, an unpolar surface functionalization is required (8,10). The challenge is to get the best of both worlds: improved dispersion of the nanofiller by an unpolar surface functionalization as well as the introduction of deep traps and tailoring of the charge trapping properties by a polar modification.

In this study, an approach is used that may provide the best balance of these improvements: designing surface-functionalized silica as shown in Figure 1. The inner layer consists of polar groups (containing nitrogen) to tailor the charge trap distribution of the nanocomposite, whereas the surface layer is composed of unpolar groups (hydrocarbon moieties) to improve the dispersion of the silica in the polymeric matrix. The polymer used in this study is a PP/propylene–ethylene copolymer blend.

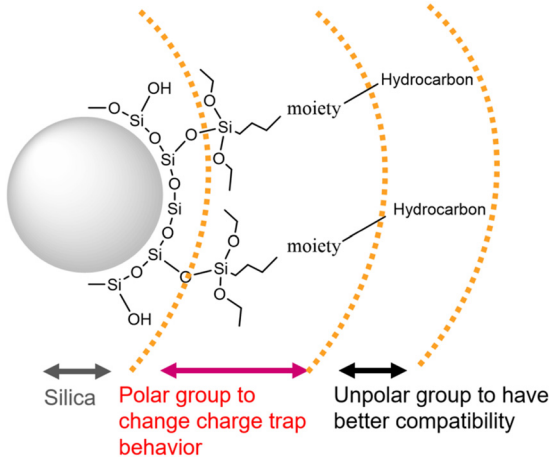

Figure 1: Scheme of the designed surface-functionalized silica.

2 Experimental

2.1 Preparation of the nanocomposites

2.1.1 Silane synthesis

To realize the surface structure sketched in Figure 1, an isocyanate silane and different alcohols were selected for the synthesis of the new silane, which will react with silica as shown in Figure 2. The reason to choose an isocyanate silane is that it can introduce deep traps into the polymeric matrix as was shown in an earlier study (11). The isocyanate group is an electrophile, thus an electron acceptor, and it is very reactive toward alcohols, which are nucleophiles and donate an electron pair. As a result, they form a urethane bridge to link both molecules as shown in Figure 3 (12).

2.1.2 Reaction of 3-(triethoxysilyl)propyl isocyanate silane (TEPI) with alcohols

The different alcohols (equimolar ratios) and TEPI were mixed in a glass flask. The flask was carefully sealed to avoid humidity. It was put into a laboratory oven at 70°C for a specified number of days as given in Table 1, until all isocyanate groups had fully reacted with the alcohol. This was detected by the disappearance of the isocyanate group band via Fourier-transform infrared spectroscopy (FTIR). The reaction schemes of all alcohols are shown in Figure 4. All alcohols and TEPI were bought from Sigma Aldrich, the Netherlands. The purities were 99.8% (ethanol), 99.5% (*tert*-butanol), 99% (cyclopentanol), 99.8% (phenyl methanol), 98% of (1-naphthalene methanol), and 95% of TEPI.

2.1.3 Silica surface modification

As a result of the reaction of TEPI with the alcohols, five new types of silanes were obtained. They are denoted as TEPI + E, TEPI + TB, TEPI + CP, TEPI + PM, and TEPI + NM1 (Figure 4). The procedure of solvent-free modification of the silica was as follows: 20 g of fumed silica and one of the silanes were mixed and stirred in a glass flask with deionized water (0.6 g) and trifluoroacetic acid (0.4 g, from

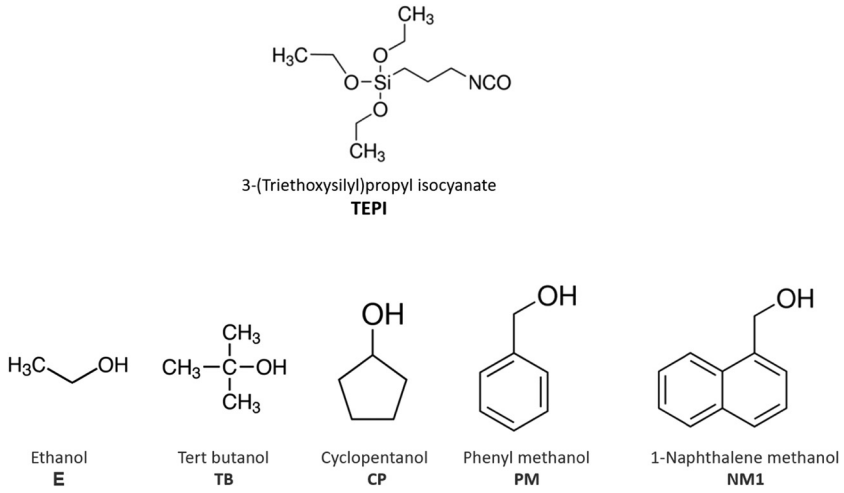

Figure 2: Chemical structures of the selected silane and alcohols.

Figure 3: Reaction of an isocyanate with alcohol.

ABCR GmbH, Karlsruhe, Germany) as a catalyst for 24 h at room temperature. Then the flask was placed in a vacuum oven for 24 h at 80°C to remove all unreacted components. The ingredients are shown in Table 2.

2.1.4 Nanocomposites manufacturing

The nanocomposites were produced by mixing PP and propylene–ethylene copolymer in a ratio of 55:45, with 2 wt% of nanosilica and 0.3 wt% of antioxidant in the Haake MiniLab Rheomix CTW5 twin screw extruder (Thermo Fisher Scientific, Waltham, MA, USA). Two types of antioxidants were used: 0.15 wt% of a phenolic one for preventing thermal oxidation of PP at higher temperatures and 0.15 wt% of a phosphite processing stabilizer. The extruder setting temperature was 230°C while the screw speed was 100 rpm and the mixing time was 4 min. After the mixing, the compounds were immediately transferred to the Haake MiniJet Pro Piston Injection Molding System (Thermo Fisher Scientific, Waltham, MA, USA; pressure 960 bar, mold temperature 60°C, injection + hold time 40 s) to prepare the final thin film of a size of 26 mm × 26 mm and a thickness of 0.5 mm.

Table 1: Reaction parameters

	20 g of TEPI				
Alcohol	E	TB	CP	PM	NM1
Weight (g)	3.7	6.0	5.6	8.7	12.8
Reaction time at 70°C (days)	7	25	8	10	35

2.2 Characterization techniques

2.2.1 FTIR of the silanes

The reaction of TEPI with the alcohols was firstly analyzed by FTIR (USA, Perkin Elmer Spectrum 100) equipped with an attenuated total reflectance unit in the range of 650–4,000 cm^{-1} to detect whether the reaction is completed, indicated by the disappearance of the isocyanate band. This took, in general, a few days.

2.2.2 Diffuse reflectance infrared Fourier-transform spectroscopy (DRIFTS) of the silicas

DRIFTS was performed on the unmodified reference silica and the modified silicas to prove the successful silica

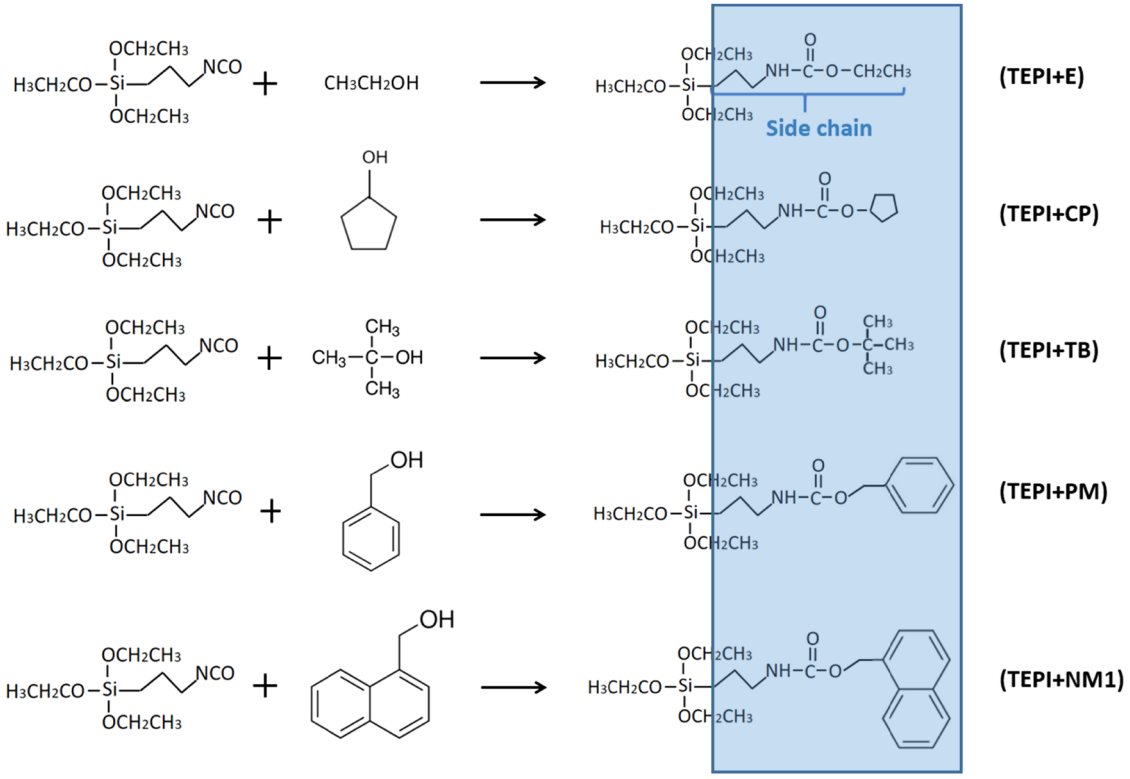

Figure 4: Scheme of reaction of TEPI with different alcohols.

Table 2: Ingredients for the modification process

	Silane (g)	Silica (g)	Water (g)	Acid (g)
TEPI + E	4.78	20	0.6	0.4
TEPI + TB	5.24			
TEPI + CP	5.24			
TEPI + PM	5.79			
TEPI + NM1	6.61			

modification with the silanes. Silica was mixed with potassium bromide for scanning. The spectra were recorded using a Perkin Elmer Spectrum 100 FT-IR Spectrometer (FTIR; Perkin Elmer – Spectrum 100 series, USA) in diffuse reflectance mode (DRIFTS). The spectra were recorded at a resolution of 4.0 cm^{-1} and averaged over 128 scans from 4,000 to 400 cm^{-1}.

2.2.3 Thermogravimetric analysis (TGA) of the silicas

TGA was performed using a TA 550 thermogravimetric analyzer (TA Instruments, USA). The measurements were performed in an atmosphere of synthetic air with a heating rate of 10°C·min^{-1}. The temperature range was ramped from ambient temperature up to 850°C.

2.2.4 Scanning electron microscopy (SEM) of the nanocomposites

The nanocomposite samples were first broken in liquid nitrogen to obtain a cross-section. This cross-section without any further treatment or coating (in order to preserve the original morphology of the samples) was investigated by SEM (Zeiss MERLIN HR-SEM, Oberkochen, Germany). To get an insight into the particle size distribution, the SEM micrographs were analyzed with the software Image J (version 1.53a, supplied by Wayne Rasband, USA). The measurement of the particle size was done manually by drawing a line with the scale. Three images of each sample were measured to get the particle size distribution.

2.2.5 Thermally stimulated depolarization current (TSDC) characterization of the nanocomposites

TSDC was applied on the nanocomposites to study their charge trapping properties. The samples were first gold coated by circular electrodes to a thickness of 100 nm and a diameter of 16 mm on both sides. The TSDC test was done by the following steps:

1. The sample was heated up to 70°C and then kept at this temperature for 5 min.
2. A direct current (DC) electric field (3 kV·mm^{-1}) was applied for 20 min.
3. The sample was quickly cooled down to −50°C under the DC electric field and stabilized for 5 min.
4. The DC electric field was removed, and the sample was short-circuited for 3 min at −50°C.
5. The sample was heated up to 130°C in a linear mode (3°C·min^{-1}). At the same time, the setup recorded the depolarization current.

3 Results and discussion

3.1 FTIR of the silanes

To track the progress of the reaction of TEPI and the alcohols, FTIR was performed. Based on the mechanism of the reaction as shown in Figure 3, the isocyanate group will vanish during the reaction. Therefore, the isocyanate band is the indicator to determine whether the reaction is completed or not. An example is presented in Figure 5: the spectra show the change of the isocyanate band at 2,284 cm^{-1} (13) with the time for the reaction of TEPI and TB. It shows that after 11 days, there is still a signal at 2,284 cm^{-1}. With increasing time, it gradually disappears until after 25 days the band is vanished, indicating that the reaction is completed. All final spectra are shown in Figure 6. The isocyanate band vanished in all cases as an evidence that the new silane was synthesized.

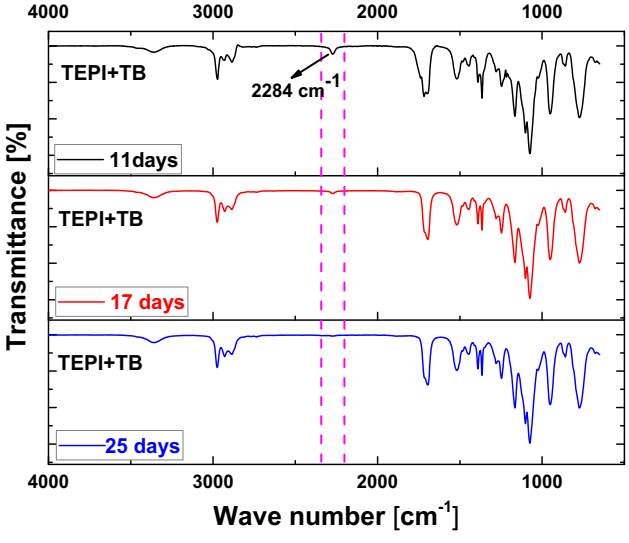

Figure 5: FTIR spectra of the mixture of TEPI and TB after 11, 17, and 25 days.

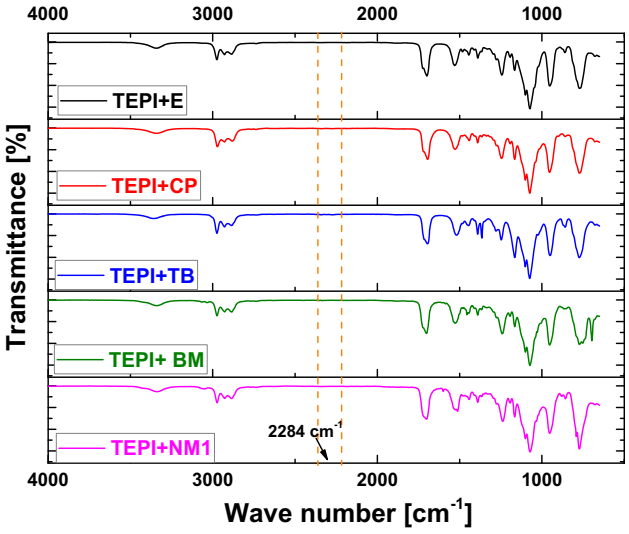

Figure 6: FTIR spectra of all synthesized silanes.

3.2 DRIFTS of the silicas

In order to prove that the silica was modified by the synthetized silanes, DRIFTS was performed, and the results are shown in Figure 7. All spectra show the broad absorbance band at a wavenumber of 1,112 cm^{-1}, resulting from the silica bulk structure of Si–O–Si stretching (14). Regarding the reference silica, the sharp band at wavenumber

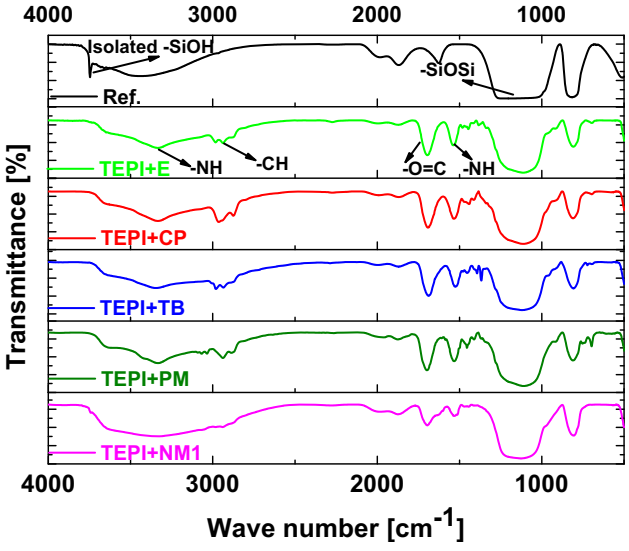

Figure 7: DRIFTS spectra of the reference (Ref.) and modified silicas.

3,700 cm^{-1} originates from the isolated silanol groups (–Si–OH), which is the indicator to determine the silica modification. This is because the isolated silanol groups on silica surface are the most reactive group and will react with the alkoxy groups from the silanes. This band vanished in all spectra of the modified silicas, proving that the silicas were successfully modified. In addition, the bands of the urethane group showed up after the silica modification. The bands at 1,700 and 1,533 cm^{-1} are stemming from the stretching of C═O and bending of N–H (15) bonds in the urethane group, respectively. A band resulting from the stretching of –NH (3,343 cm^{-1}) in the urethane group also appeared in the modified silicas. Moreover, the –CH stretching bands from hydrocarbon chains appear in the range from 2,970 to 2,880 cm^{-1}. The absorbance bands of both, urethane and alkyl groups, further prove that the silica is successfully modified by the synthetized silanes. Additionally, one can also observe that the bands of the urethane and alkyl moieties are weak in the spectrum of TEPI + NM1, which indicates a lower modification level than for the other modified silicas.

3.3 Thermogravimetrical analysis (TGA) of silicas

To further study the modification of the silica surface, TGA was performed to quantitatively investigate the deposition level. The TGA results are presented in Figure 8. It

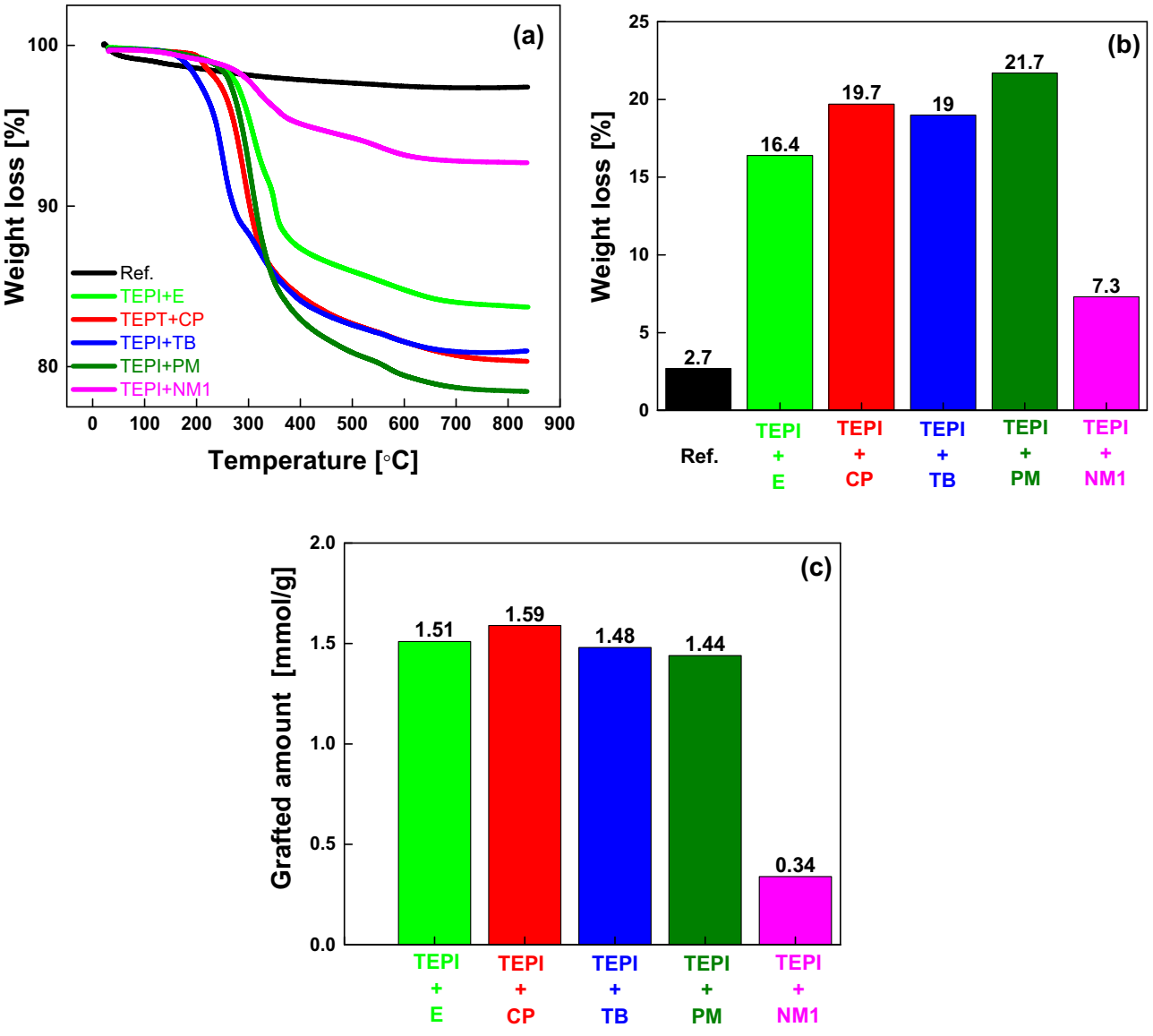

Figure 8: TGA curves of the reference silica and modified silicas (a), weight loss up to a temperature of 850°C (b), and molar grafting effectiveness of the silanes (c).

is clearly shown that the surface-modified silicas exhibit higher weight losses than the reference silica. The weight loss of the modified silicas is ascribed to the removal of the organic molecules from the silica surface, indicating the successful modification of the silica with the synthetized silanes.

To further investigate the degree of modification of the five designed silicas, the molar amount of the grafted molecules was calculated based on Eq. 1, similar to (11):

$$\text{Grafted amount } (\text{mmol} \cdot \text{g}^{-1}) = \frac{10^3 W}{M(100 - W)} \quad (1)$$

where W is the weight loss (%) of the modified silica measured by TGA; M is the molecular weight of the side chain of the synthetized silanes (130 g·mol^{-1} – side chain of TEPI + E; 154 g·mol^{-1} – side chain of TEPI + CP; 158 g·mol^{-1} – side chain of TEPI + TB; 192 g·mol^{-1} – side chain of TEPI + PM; and 232 g·mol^{-1} – side chain of TEPI + NM1, and the side chains of the new silanes are indicated in Figure 4).

Almost no weight loss below a temperature of 200°C was measured for any of the five modified silicas, which means that there is very less water or unreacted ethoxy groups present in the modified silicas. Therefore, we assumed that all weight loss of the modified silicas stems from the removal of the organic side chain ($-CH_2-CH_2-CH_2-$NHCO-hydrocarbon) of the silanes. The calculated values of the grafted amount of the silane are shown in Figure 8c. It is clearly seen that TEPI + E, TEPI + CP, TEPI + TB, and TEPI + PM show a similar grafting density due to similar molecular mobility of the silanes during the modification. However, the TEPI + NM1 sample shows a very low grafting density due to the high molecular weight and potentially high intermolecular interactions (due to the flat molecule structure of the naphthalene and Π–Π stacking) of the silane leading to a low molecular mobility, resulting in a low degree of the modification. Despite the different weight loss and related grafted densities of the modified silicas, it can still be concluded that the designed structure of the silicas (Figure 9) was successfully realized through the solvent-free modification.

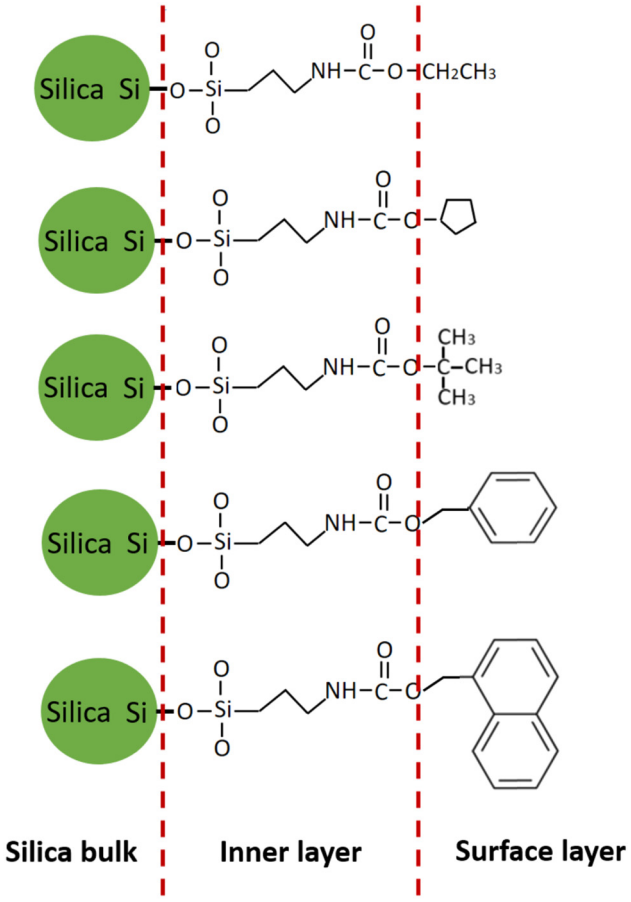

Figure 9: Chemical structure of the surface-modified silicas.

3.4 SEM of the nanocomposites

After modification of silica with the designed silanes (inner layer + surface layer), the nanocomposites were prepared through mini-injection molding. One of the reasons to modify silica by the designed structures was to improve the compatibility with the polymer resulting in better dispersion of the silica in the polymeric matrix. Therefore, SEM was performed on the cross-sections of the nanocomposites filled with the reference and modified silicas, as shown in Figure 10. In the nanocomposite filled with the reference silica, large size clusters are present. This is due to the fact that the reference silica has a very polar surface and is therefore not compatible with the polymer matrix exhibiting an unpolar nature. The nanocomposites filled with the modified silicas clearly show a much better dispersion of the filler, without large clustering, than the one filled with the reference silica. To get an insight into the particle size distribution, several SEM micrographs were analyzed with the software Image J (version 1.53a, supplied by Wayne Rasband, USA). The histograms of the particle size distributions are shown in Figure 11. The reference silica shows a broad size distribution in a range of 80–5,000 nm, and most clusters are above 300–400 nm in diameter. For the modified silicas, smaller size clusters as well as a narrower size distribution are seen. The mean size of the modified silica clusters is around 100 nm in diameter. This proves that the modification improves the nanosilica dispersion and

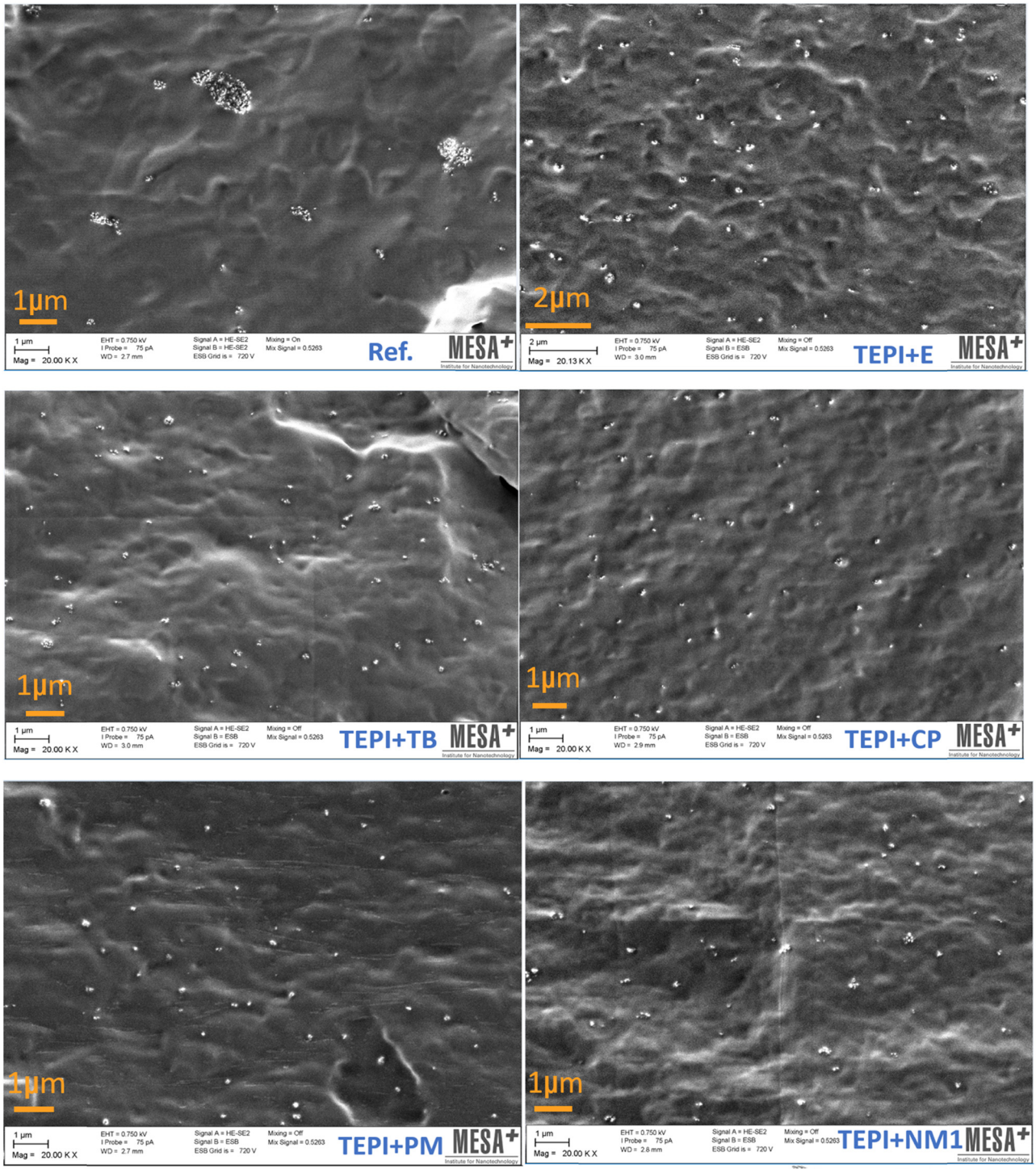

Figure 10: SEM images of nanocomposites filled with reference silica or modified silicas.

distribution in the polymer matrix. Although the polar urethane group is introduced on the silica surface, the surface layer of the modified silica with the unpolar hydrocarbon group improves the compatibility of the silica with the unpolar polymer matrix.

3.5 TSDC

To compare the effect of the reference silica and the modified silicas on the charge trapping properties of the PP/propylene–ethylene copolymer blend, TSDC

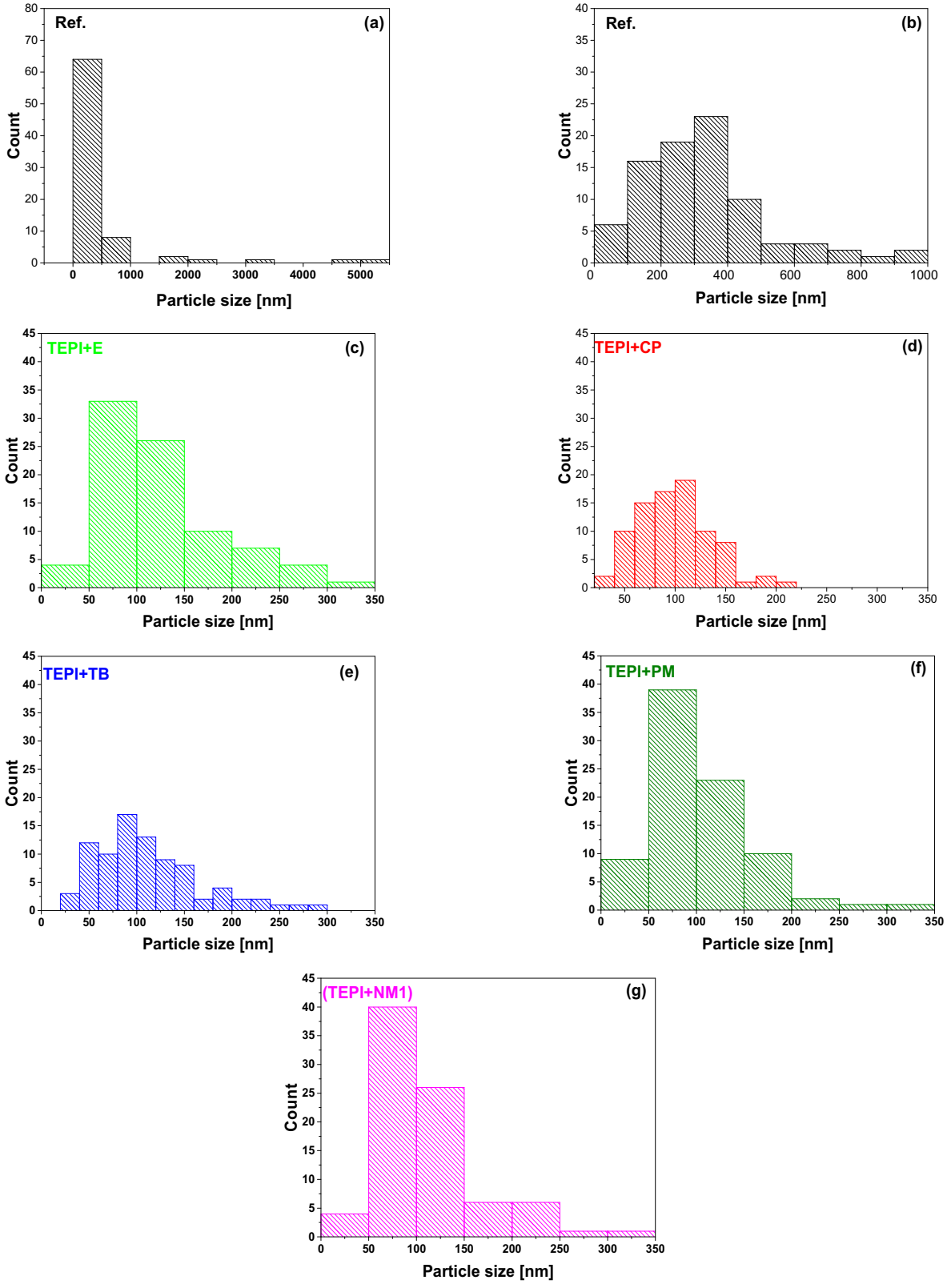

Figure 11: Histograms of the cluster size distribution for the reference silica and the modified silicas in the polymer matrix. (a) and (b) Represent the reference silica cluster size distribution. (c) Represents the TEPI + E modified silica cluster size distribution. (d) Represents the TEPI + CP modified silica cluster size distribution. (e) Represents the TEPI + TB modified silica cluster size distribution. (f) Represents the TEPI + PM modified silica cluster size distribution. (g) Represents the TEPI + NM1 modified silica cluster size distribution.

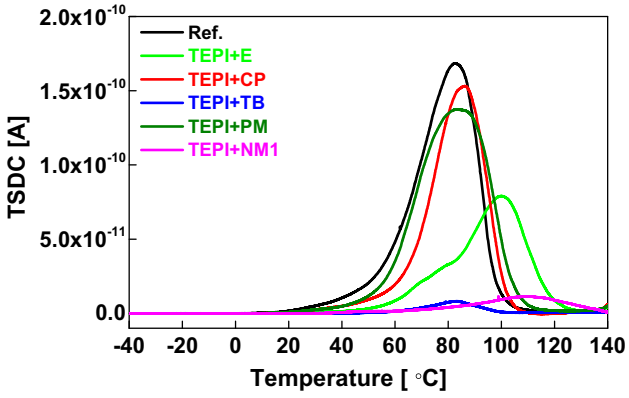

Figure 12: TSDC spectra of the nanocomposites filled with the reference silica and the modified silicas.

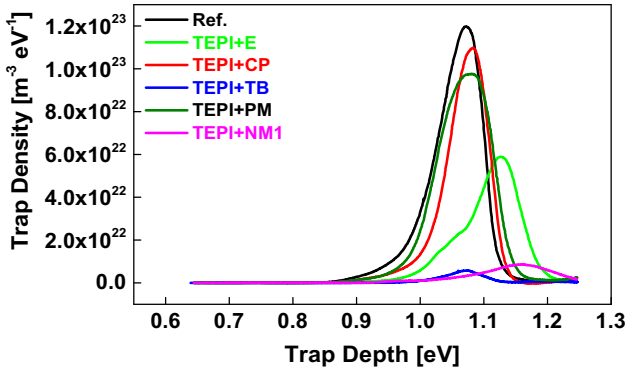

Figure 13: Calculated trap density and depth of the nanocomposites filled with the reference silica and the modified silicas.

measurements were performed, and the results are presented in Figure 12. The calculated trap depth and trap density by using a numerical method (16) are shown in Figure 13. The relaxation of the trapped charges contributes to the current during the thermal depolarization process. The TSDC temperature and current intensity are associated with the trap depth and density, respectively. The TSDC main peak temperatures and current intensities of the composites are shown in Table 3. Compared to the reference silica, the TSDC peak temperature of the composites filled with the modified silicas moves to higher values, indicating deeper charge traps. This is due to the introduced polar moieties in the inner layer of the modified silicas. The samples filled with the designed silicas also show a lower TSDC peak intensity, indicating a lower trap density. Among all the samples, the sample filled with TEPI + NM1 shows the highest TSDC peak temperature (the deepest charge traps), whereas the sample with TEPI + TB exhibits the lowest TSDC current intensity (the lowest trap intensity).

In addition, it is also found that both TEPI + TB and TEPI + E exhibit quite different effects on the charge trap distribution of the composites as shown in Figure 14, even though, TEPI + TB is similar to TEPI + E from a chemical point of view. This is due to two effects:

- *The shielding effect*: *tert*-Butyl groups exhibit a better shielding effect than ethyl groups (17). The shielding effect can hinder the charge moving to the silica surface, which contributes to traps being less accessible for charges on the silica surface. This leads to a lower apparent trap density in the sample filled with TEPI + TB in comparison to the one containing TEPI + E.
- *The formation of deep traps*: There is an indication of a small number of deep traps located at an energy of 1.2 eV in the samples filled with TEPI + TB as shown in Figure 14. The charges trapped inside these traps cannot detrap easily, and a local electrical field is formed, as a result, hindering the further charge injection into the sample. Consequently, a lower apparent trap density is present for the sample filled with TEPI + TB than for the one filled with TEPI + E.

To further study the TSDC results, the amount of injected charges during polarization and the released charges during the depolarization were calculated by integrating the area under the current versus time curves. The calculated results are presented in Figure 15. With regard to the injected charges, the samples filled with the reference, TEPI + CP, and TEPI + PM silica all show a similar amount of injected charges, whereas the samples filled with TEPI + E, TEPI + TB, and TEPI + NM1 show a lower amount. In the case of released charges, the samples present the same trend as for injected charges. The injected charges are related to the charge trap distribution in the sample. Although we have observed a deeper trap with lower intensity in all samples filled with the

Table 3: TSDC main peak temperature and peak intensity

	Ref.	TEPI + E	TEPI + TB	TEPI + CP	TEPI + PM	TEPI + NM1
TSDC peak temperature (°C)	82.6	100.1	83.1	86.1	83.2	110.3
TSDC peak intensity (*A*)	1.88×10^{-10}	0.79×10^{-10}	0.08×10^{-10}	1.53×10^{-10}	1.37×10^{-10}	0.11×10^{-10}

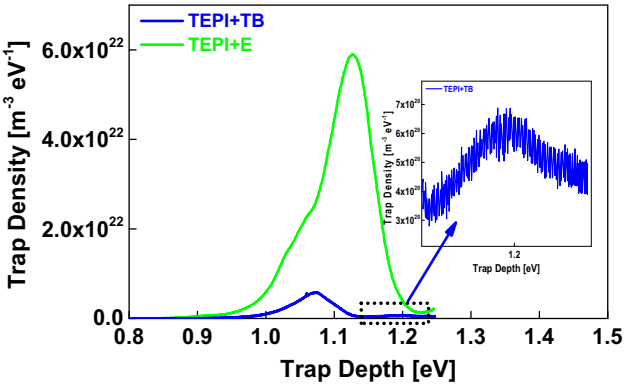

Figure 14: TSDC spectra of the nanocomposites filled with the TEPI + E and the TEPI + TB.

designed silicas compared to the one containing the reference silica, the changes for the sample filled with TEPI + CP and TEPI + PM are small, their charge trap depth is only slightly deeper, and the trap density is slightly lower than the reference composite. In the case of TEPI + TB, the peak intensity is much lower than the one of the reference composites, and it also contains a small amount of the deep traps as shown in Figure 14. Both contributing to the low number of injected charges. For the TEPI + E and TEPI + NM1 composites, the TSDC peak temperature is 17.5°C and 27.7°C higher than for the sample containing the reference silica. This means that the traps present in the samples filled with TEPI + E and TEPI + NM1 are much deeper than the traps in the reference composite. In our previous study, we have observed that a sample with deep traps can block further charge injection, resulting in a low amount of injected charges (11). The charges caught by the deep traps are not easily detrapped and require additional energy support. The trapped charge will repel the further charge injection from the electrode. Therefore, the amount of injected charges to the samples filled with the TEPI + E and TEPI + NM1 is low due to the deep traps introduced by the corresponding silicas. In addition, the low TSDC peak intensity indicating low trap density also contributes to the low amount of injected charges for the TEPI + E and TEPI + NM1 silica-filled samples.

In summary, charge trap depth and density can influence charge injection. The samples with very deep traps show a low level of injected charges and see the samples filled with TEPI + E or TEPI + NM1. Furthermore, a sample with less deep traps but with very low trap density can also result in low charge injection, as in the case of the sample filled with the TEPI + TB-modified silica.

To estimate the conductivity of the studied nanocomposites, the charging current density during isothermal polarization is measured and presented in Figure 16. Although it is clear that not all the samples reached the steady state DC conductivity current due to the short poling time (20 min), the difference in the charging current behavior between all the studied samples is apparent. The initial charging current is related to the fast polarization mechanisms. After the initial current transient, the slowly decaying current over time results from several factors (18): (a) electrode polarization, (b) dipole orientation, (c) charge storage leading to trapped space charge effects, (d) tunneling of the charge carriers from the electrodes, and (e) hopping of the charge carriers through localized states. Taking the same electrode for all the tests and the same nonpolar polymer into consideration, the electrode polarization and dipole orientation can be neglected when comparing these samples. Hence, the absolute current level and the decay rate

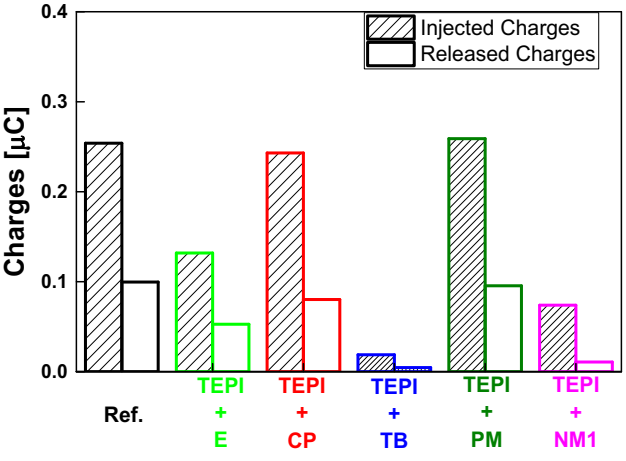

Figure 15: Calculated amount of injected and released charges.

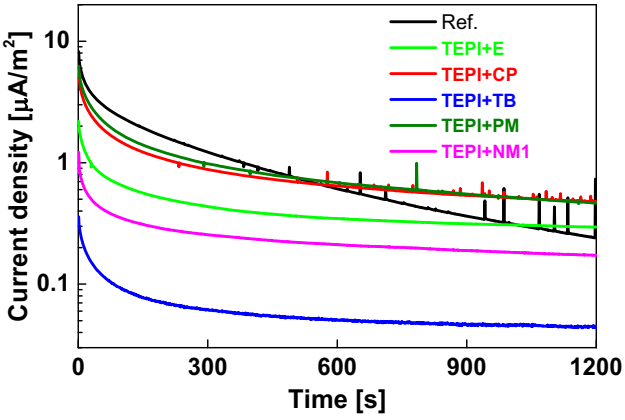

Figure 16: Charging current density during the isothermal polarization process.

of the charging current over time can convey information on the charge build-up (related to the occupied trap density) and charge mobility (related to the trap depth) in the samples.

The sample filled with the reference silica exhibits a slow current decay behavior and higher current density than the other samples measured during the 20 min of poling time, implying a high amount of occupied traps or a shallower trap depth (see Figure 13). In the case of the composites filled with the modified silicas, especially with the TEPI + TB sample, a rapid decay and very low current density indicate rapid trapping, a low number of trap sites, and buildup of homocharge in deep traps. The deep traps can hinder the charge injection from the electrode and hence decreasing the charging current magnitude and indicating a low amount of occupied traps in this sample as well.

Nevertheless, among all these samples, the sample filled with TEPI + TB-modified silica exhibits a very low current density, indicating low transient conductivity characteristics. It should be stressed that this test was only done at a low electrical field of 3 $kV \cdot mm^{-1}$ at 70°C, and it cannot represent the electrical behavior under a high electrical field and at other temperatures. However, these preliminary results already provide valuable information: The TEPI + TB-modified silica result in a good dispersion as shown in Figures 10 and 11, and the lowest amount of charge injection (Figure 14) under 3 $kV \cdot mm^{-1}$ at 70°C, indicating to be a potential candidate for HVDC cable insulation application. To further prove the applicability of this silica, more studies under high electric fields and at different temperatures are necessary.

4 Conclusion

Five designed surface-functionalized silicas were successfully synthetized. The designed silicas and the unmodified reference silica were compounded with the PP/propylene–ethylene copolymer to produce the nanocomposites via injection molding.

The modified silicas exhibit a better dispersion than the unmodified reference one. The designed silicas introduce deeper traps with a lower trap density than the reference filler in the nanocomposite. However, the charge trap depth level and densities are different for the silica composites containing the modified silicas. The samples filled with silica modified with TEPI + CP and TEPI + PM show a trap distribution close to the one of the reference samples. As a result, the amount of injected charges and the charging current densities of these three composites are similar. In contrast to this, the TEPI + E and TEPI + NM1-modified silicas introduce much deeper traps than the reference silica, leading to a low current density and low amount of charge injection. In the case of the sample filled with the TEPI + TB, it shows the lowest charging current density and smallest charge injection, indicating low conductivity and space charge injection, probably as a result of the low trap density and a small amount of deep traps in the sample under 3 $kV \cdot mm^{-1}$ at 70°C. Additionally with the good dispersion of the TEPI + TB-modified silica, the sample filled with this silica is a potential candidate for application in HVDC cable insulation material. As mentioned before, the TSDC test and current density are done only at low electrical fields. Wide characterizations on different elelctrical fields and temperatures including breakdown test, aging, and space charge measurement are needed to evaluate the overall performance of HVDC insulation material in the future.

Acknowledgements: The authors also would like to thank Evonik Industries for providing a free silica sample.

Funding information: This project has received funding from the European Union's Horizon 2020 research and innovation program under grant agreement No. 720858.

Author contributions: Xiaozhen He: formal analysis, investigation, resources, writing – original draft, writing – review and editing, and visualization; Ilkka Rytöluoto: investigation, writing – review and editing; Rafal Anyszka: writing – review and editing; Amirhossein Mahtabani: formal analysis; Minna Niittymäki: investigation; Eetta Saarimäki: investigation; Christelle Mazel: resources; Gabriele Perego: resources; Kari Lahti: writing – review and editing; Mika Paajanen: project administration; and Wilma Dierke: supervision, writing – review and editing; and Anke Blume: supervision.

Conflict of interest: Authors state no conflict of interest.

References

(1) Nelson JK, Fothergill JC, Dissado LA, Peasgood W. Towards an understanding of nanometric dielectrics. Annual Report Conference on Electrical Insulation and Dielectric Phenomena IEEE, Mexico; 2002 Oct 20–24. p. 295–8.

(2) Zhou Y, Dang B, Wang H, Liu J, Li Q, Hu J, et al. Polypropylene-based ternary nanocomposites for recyclable high-voltage direct-current cable insulation. J Compos Sci. 2018;165:168–74.

(3) Pourrahimi AM, Pallon LK, Liu D, Hoang TA, Gubanski S, Hedenqvist MS, et al. Polyethylene nanocomposites for the next generation of ultralow-transmission-loss HVDC cables: insulation containing moisture-resistant MgO nanoparticles. ACS Appl Mater Interfaces. 2016;8(23):14824–35.
(4) Roy M, Nelson JK, MacCrone RK, Schadler LS, Reed CW, Keefe R. Polymer nanocomposite dielectrics-the role of the interface. IEEE Trans Dielectr Electr Insul. 2005;12(4):629–43.
(5) Green C, Vaughan A. Nanodielectrics-How much do we really understand? IEEE Electr Insul Mag. 2008;24(4):6–16.
(6) Min D, Cui H, Hai Y, Li P, Xing Z, Zhang C, et al. Interfacial regions and network dynamics in epoxy/POSS nanocomposites unravelling through their effects on the motion of molecular chains. J Compos Sci. 2020;199:108329.
(7) Roy M, Nelson JK, MacCrone RK, Schadler LS. Candidate mechanisms controlling the electrical characteristics of silica/XLPE nanodielectrics. J Mater Sci. 2007;42(11):3789–99.
(8) Liu D, Pourrahimi AM, Olsson RT, Hedenqvist MS, Gedde UW. Influence of nanoparticle surface treatment on particle dispersion and interfacial adhesion in low-density polyethylene/aluminium oxide nanocomposites. Eur Polym J. 2015;66:67–77.
(9) Mahtabani A, Rytöluoto I, Anyszka R, He X, Saarimäki E, Lahti K, et al. On the silica surface modification and its effect on charge trapping and transport in pp-based dielectric nanocomposites. ACS Appl Polym Mater. 2020;2(8):3148–60.
(10) He X, Rytöluoto I, Anyszka R, Mahtabani A, Saarimäki E, Lahti K, et al. Surface modification of fumed silica by plasma polymerization of acetylene for PP/POE blends dielectric nanocomposites. Polymers. 2019;11(12):1957.
(11) He X, Rytöluoto I, Anyszka R, Mahtabani A, Saarimäki E, Lahti K, et al. Silica surface-modification for tailoring the charge trapping properties of PP/POE based dielectric nanocomposites for HVDC cable application. IEEE Access. 2020;8:87719–34.
(12) Bacaloglu R, Cotarca L, Marcu N, Tölgyi S. Kinetics and mechanism of isocyanate reactions. II. Reactions of aryl isocyanates with alcohols in the presence ob tertiary amines. J Prakt Chem. 1988;330(4):530–40.
(13) Xu L, Li C, Ng KS. In-situ monitoring of urethane formation by FTIR and Raman spectroscopy. J Phys Chem A. 2000;104(17):3952–7.
(14) Huang J, Zhang L, Tang Z, Wu S, Guo B. Reprocessable and robust crosslinked elastomers via interfacial CN transalkylation of pyridinium. J Compos Sci. 2018;168:320–6.
(15) Nouri N, Rezaei M, Sofla RLM, Babaie A. Synthesis of reduced octadecyl isocyanate-functionalized graphene oxide nanosheets and investigation of their effect on physical, mechanical, and shape memory properties of polyurethane nanocomposites. J Compos Sci. 2020;194:108170.
(16) Tian F, Bu W, Shi L, Yang C, Wang Y, Lei Q. Theory of modified thermally stimulated current and direct determination of trap level distribution. J Electrostat. 2011;69:7–10.
(17) Kawamura A, Ueno S, Takai C, Takei T, Razavi-Khosroshahi H, Fuji M. Effect of steric hindrance on surface wettability of fine silica powder modified by n- or t-butyl alcohol. Adv Powder Technol. 2017;28(10):2488–95.
(18) Gupta DD, Brockley RS. A study of'absorption currents' in low-density polyethylene. J Phys D Appl Phys. 1978;11(6):955.